145400-3-S1

ASTRONOMICAL IMAGING BY PROCESSING STELLAR SPECKLE INTERFEROMETRY DATA

J.R. FIENUP and G.B. FELDKAMP

Published in the Proceedings of the SPIE 243-16
Applications of Speckle Phenomena,
San Diego, California, July 30, 1980.

ENVIRONMENTAL
RESEARCH INSTITUTE OF MICHIGAN
BOX 8618 • ANN ARBOR • MICHIGAN 48107

Astronomical imaging by processing stellar speckle interferometry data

J.R. Fienup and G.B. Feldkamp

Environmental Research Institute of Michigan
Radar and Optics Division
P.O. Box 8618, Ann Arbor, Michigan 48107

Abstract

Diffraction-limited images, of resolution many times finer than what is ordinarily obtainable through large earth-bound telescopes, can be obtained by first measuring the modulus of the Fourier transform of an object by the method of Labeyrie's stellar speckle interferometry, and then reconstructing the object by an iterative method. Before reconstruction is performed, it is first necessary to compensate for weighting functions and noise in order to arrive at a good estimate of the object's Fourier modulus. A simple alternative to Worden's method of compensation for the MTF of the speckle process is described. Experimental reconstruction results are shown for the binary star system SAO 94163.

Introduction

As discussed in several papers in this session on Stellar Speckle Interferometry, Labeyrie's method[1] of processing many short-exposure images can be used to arrive at a diffraction-limited estimate of the Fourier modulus of an astronomical object despite the presence of atmospheric turbulence. Since the diffraction limit of a large-aperture telescope is many times finer than the resolution ordinarily obtainable through the atmosphere at optical wavelengths, stellar speckle interferometry has the potential for providing images having many times finer detail than what is ordinarily obtainable from earth-bound telescopes. Unfortunately, except for special cases in which an unresolved star is very near the object of interest[2], the Fourier modulus data can be used to directly compute only the autocorrelation of the object and not the object itself. In recent years, it has been shown that this stumbling block can be overcome by an iterative method[3] of computing the object's spatial (or angular) brightness distribution, which uses the Fourier modulus data provided by stellar speckle interferometry combined with the a priori knowledge that the object distribution is nonnegative. This method provides an alternative to other fine-resolution imaging techniques[4,5].

In the remainder of this paper, stellar speckle inteferometry and the iterative reconstruction method are briefly reviewed. Then more detailed discussions of noise terms and MTF factors present in speckle interferometry are given, and methods of obtaining an improved estimate of an astronomical object's Fourier modulus are described. Finally, some recent results obtained with telescope data are shown.

Basic stellar speckle interferometry

Labeyrie's stellar speckle interferometry starts by taking a number of short-exposure images of an astronomical object:

$$d_m(x) = f(x) \ast s_m(x) \tag{1}$$

where $f(x)$ is the spatial or angular brightness distribution of the object and $s_m(x)$ is the point-spread function due to the combined effects of atmosphere and the telescope for the m^{th} exposure. The coordinate x is a two-dimensional vector and $\ast$ denotes convolution. It is assumed that the exposure time is short enough to "freeze" the atmosphere and only a narrow spectral band is used. The Fourier transform of each short-exposure image is computed:

$$D_m(u) = \int_{-\infty}^{\infty} d_m(x) \exp(i2\pi ux)\, dx \tag{2}$$

In this paper, capital letters will denote the complex Fourier transforms of the corresponding lower-case letters, and the coordinate u is referred to as a spatial frequency. The summed squared Fourier modulus (the summed power spectrum) is computed:

$$\sum_{m=1}^{M} |D_m(u)|^2 = \sum_{m=1}^{M} |F(u)S_m(u)|^2 = |F(u)|^2 \sum_{m=1}^{M} |S_m(u)|^2 \tag{3}$$

The factor $\sum|S_m(u)|^2$ can be thought of as the square of the MTF of the speckle interferometry process (the speckle MTF^2) and it can be determined approximately by performing stellar speckle interferometry on an isolated unresolved star through atmospheric conditions having the same statistics as those through which the object imagery is taken. Dividing the summed power spectrum by the speckle MTF^2 yields, according to Eq. (3), $|F(u)|^2$, the squared Fourier modulus of the object.

Since it is simply the Fourier transform of $|F(u)|^2$, the autocorrelation of the object can be obtained by Labeyrie's method. However, the autocorrelation gives only very limited information about the object: its diameter, and the separation for the case of a binary star system. Only for the special cases of (1) an object known to be centro-symmetric and (2) an object having an isolated unresolved star within the same isoplanatic patch[2] (within a few seconds of arc) can the autocorrelation, or equivalently $|F(u)|^2$, be used to directly compute the object.

The iterative method

We have, in addition to the measured Fourier modulus, the a priori knowledge that the object brightness is a real, nonnegative function. The reconstruction problem consists of finding a nonnegative object that is consistent with the measured Fourier modulus data. This problem can be solved by the iterative method depicted in Figure 1. It consists of

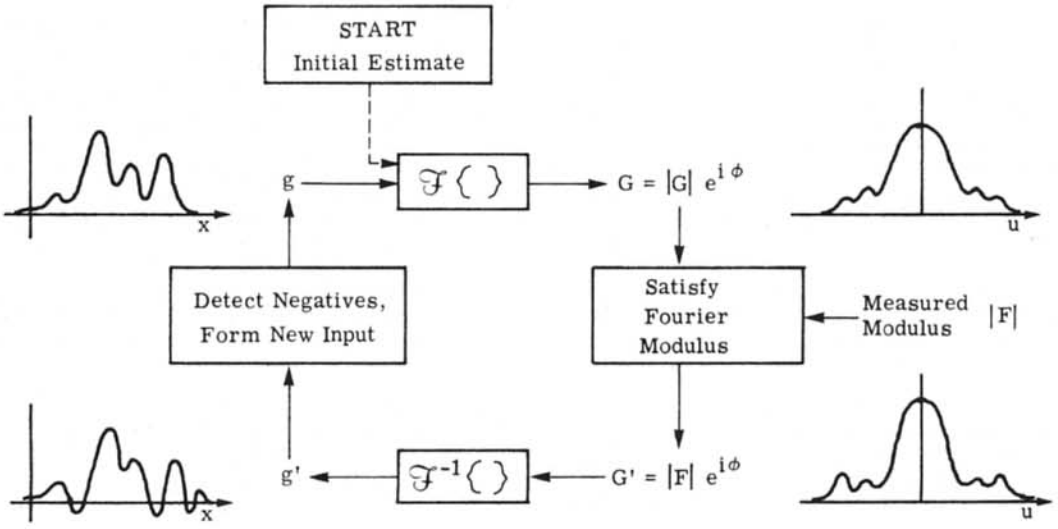

Figure 1. Iterative processing overview.

four steps: (1) an initial estimate of the object, g(x) (which we usually choose to be a field of random numbers), is Fourier transformed; (2) in the Fourier domain, the measured Fourier modulus is substituted for the computed Fourier modulus, and the computed phase is unaltered; (3) the result is inverse Fourier transformed, yielding an image g'(x); and (4) a new g(x) is chosen, based on the violation of the object-domain constraints by g'(x). The four steps are repeated until the mean-squared error is reduced to a small value consistent with the signal-to-noise ratio of the measured Fourier modulus data. The mean-squared error in the image domain is

$$E_o^2 = \frac{\int_\gamma [g'(x)]^2\,dx}{\int_{-\infty}^{\infty} [g'(x)]^2\,dx} \tag{4}$$

where the region γ includes all points at which g'(x) violates the object domain constraints (where it is negative or possibly where it exceeds an a priori known diameter). Several different methods for choosing a new g(x) have proven successful. For the results shown in this paper, we used for most iterations

$$g_{k+1}(x) = \begin{cases} g'_k(x) & , \quad x \notin \gamma \\ g_k(x) - .5g'_k(x), & x \in \gamma \end{cases} \tag{5}$$

interspersing with

$$g_{k+1}(x) = \begin{cases} g'_k(x), & x \notin \gamma \\ 0 \quad , & x \in \gamma \end{cases} \tag{6}$$

every few iterations, where the subscript k refers to the k^{th} iteration and γ is defined as in Eq. (4). More detailed discussions of the iterative method and why it works can be found in References 3 and 6.

For the binary star results shown later, when random numbers were used for the initial input, then over a hundred iterations were required for an array size of 128 x 128 pixels (about the same number of iterations that has been required for complicated two-dimensional objects), taking about two minutes on a Floating Point Systems AP 120B array processor. When a binary star pattern with the correct spacing (which can be determined from the autocorrelation) but the incorrect brightness ratio was used as the initial input, then only a dozen iterations were required for convergence, taking about 10 seconds. It was found that the nonnegativity constraint was sufficient, and the diameter constraint was not needed.

Noise and MTF characteristics and their compensation

The data used for the experiments described here were obtained from the Steward Observatory Speckle Interferometry Program which is described in more detail elsewhere in this proceedings volume[7]. For this "event detection" data, it is assumed that any one short exposure image contains no more than one photon in any one pixel (and most pixels record zero photons). After an image is magnified, intensified, and detected, (among other things) it is thresholded to produce an image consisting of ones (where above the threshold) and zeros. Each image is autocorrelated, and the sum of all the autocorrelations is computed. The summed power spectrum is computed as the Fourier transform of the summed autocorrelation. In addition, each image is centroided (translated to make their centroids coincident) to within the nearest pixel, and the sum of the centroided images is computed.

The telescope diameter is 2.3 meters; and, for 30X magnification of the image, the image scale is approximately 0.02 arc-sec per pixel along each line, and is about 0.017 arc-sec per line (it is stretched by about 13% in that dimension relative to the along-line dimension). For 60X magnification, the scale is half that. The data is digitized in 256 x 256 arrays.

Figure 2 shows an example of a cut through the summed power spectrum of an unresolved star, SAO 36615. This data was taken at 60X magnification (0.01 arc-sec per pixel = 4.7×10^{-8} radians per pixel) at a 30 nm wavelength band centered at 750 nm. The scale in the Fourier domain is 750 nm/(4.7×10^{-8} rad x 256) = 0.062 meters (of telescope aperture) per pixel. For a telescope diameter of 2.3 meters, the highest spatial frequency passed by the telescope aperture is 2.3 m/(0.062 m/pix) = 37 pixels from zero frequency. Ideally (no atmosphere or aberrations and no noise), the summed power spectrum of an unresolved star would be the square of the MTF due to the telescope aperture (that MTF is the autocorrelation of the telescope pupil function). Assuming a circular aperture, a cut through the telescope aperture MTF would have a roughly cone shape[8] and be zero beyond pixel 37. However, the summed power spectrum of the unresolved star shown in Figure 2 is very far from this ideal.

Two effects dominate the shape of the power spectrum. First, the speckle MTF^2, mentioned earlier in connection with Eq. (3), drops very rapidly for the very low spatial frequencies near the atmospheric cut-off. This results in the spike-like behavior of the summed power spectrum for very low spatial frequencies. Beyond the very low spatial-frequency region, the speckle MTF^2 is much better behaved and decreases slowly[9]. Second, photon noise results in, among other things, a noise bias term in the summed power spectrum[10]. This noise bias term dominates in the higher spatial frequencies. Beyond a radius of 37 pixels in the summed power spectrum, no signal energy exists -- it is purely noise. They so dominate the summed power spectrum that little useful information can be obtained unless compensation is made for both of these two effects.

The noise bias term and the detection transfer function

One would ordinarily eliminate the noise bias term simply by subtracting a constant from the summed power spectrum[10,11]. However, as seen from Figure 2, the noise bias term, which is seen by itself beyond pixel 37, is not a constant in this case. This results from the fact that upon detection and thresholding, a single photon sometimes results in more than one pixel recording a one, depending upon the threshold level and the size of the splotch of light exiting from the image intensifier. Table 1 shows the autocorrelations and the individual squared transfer functions of some of the various patterns of ones resulting from a single photon. Each pattern is, in effect, the impulse response of the de-

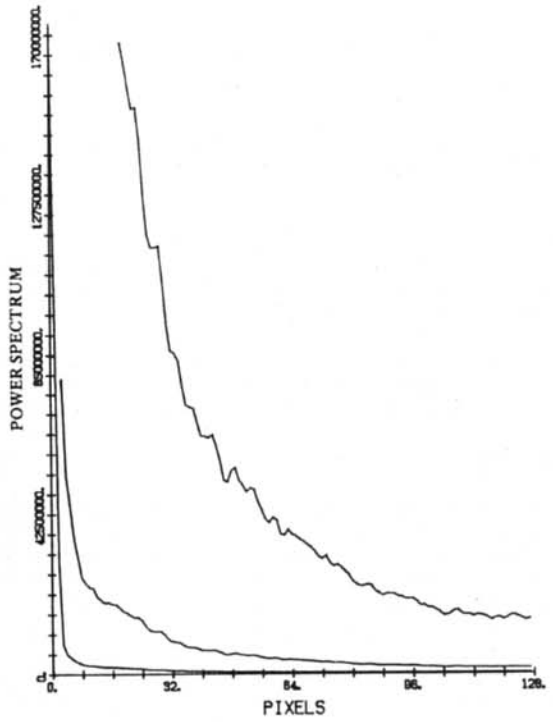

Figure 2. Summed power spectrum of an unresolved star (linear scale). The middle and upper curves are the same as the lower curve, except have 10X and 100X vertical scales, respectively.

Table 1. Event detection data: individual impulse responses, their auto correlations, and their power spectra.

DETECTION IMPULSE RESPONSE	AC OF IMPULSE RESPONSE	DETECTION TRANSFER FUNCTION^2
1	1	1
1 1	1 2 1	$2 + 2\cos(2\pi\, u/N)$
1 / 1	1 / 2 / 1	$2 + 2\cos(2\pi\, v/N)$
1 1 1	1 2 3 2 1	$3 + 4\cos(2\pi\, u/N) + 2\cos(4\pi\, u/N)$
1 / 1 1	1 1 / 1 3 1 / 1 1	$3 + 2\cos(2\pi\, u/N) + 2\cos(2\pi\, v/N) + 2\cos[2\pi(u+v)/N]$
⋮	⋮	⋮

tection system; and in any one image, several different patterns may appear. That is, this impulse response may vary from photon to photon within the same image. Assuming a sparse population of photons within each image, it can be shown that the net squared transfer function, due to the ensemble of photon-produced patterns within an image, is given by a weighted sum of the individual squared transfer functions of the individual patterns. We refer to this weighted sum as the detection transfer function squared (DTF^2).

One can compensate for the noise bias term by the following steps[12]. (1) Over the spatial frequencies above the telescope cut-off, perform a two-dimensional least-squares fit of a weighted sum of individual squared transfer functions (some of which are shown in Table 1) to the summed power spectrum. By this, the DTF^2 is determined. (2) Compensate the effects of the DTF^2 by dividing the summed power spectrum by the DTF^2 (for all spatial frequencies). By this, the noise bias term is made a constant. (3) Subtract from the DTF^2-compensated summed power spectrum the constant noise bias term. This DTF^2 and noise bias compensation are demonstrated in Figures 3 and 4 for the binary star system SAO 94163. In this case, the magnification was 30X and the wavelength was 750 nm (10 nm spectral bandwidth) and so the telescope cut-off is at a spatial frequency of 74 pixels. This data set resulted from power-spectrum averaging of 1820 short exposure images containing a total of about 2.4×10^5 photons.

In the autocorrelation domain, the noise bias term results in a spike at the (0, 0) coordinate, and the DTF^2 causes the spike to be spread over a few pixels about (0, 0). Compensation for the DTF^2 causes the spike to collapse to a delta-function at (0, 0). Then the subtraction of the noise bias in the Fourier domain removes the delta-function at (0, 0) in the autocorrelation.

More generally, the functional form of the DTF^2 is heavily dependent on the manner in which the images are detected and should be modified according to the characteristics of the detection hardware used.

The speckle MTF^2

Compenstion for the speckle MTF^2 would ordinarily be accomplished by dividing the summed power spectrum by the summed power spectrum of a reference star[1]. Both power spectra should first be corrected for the DTF^2 and the noise bias term.

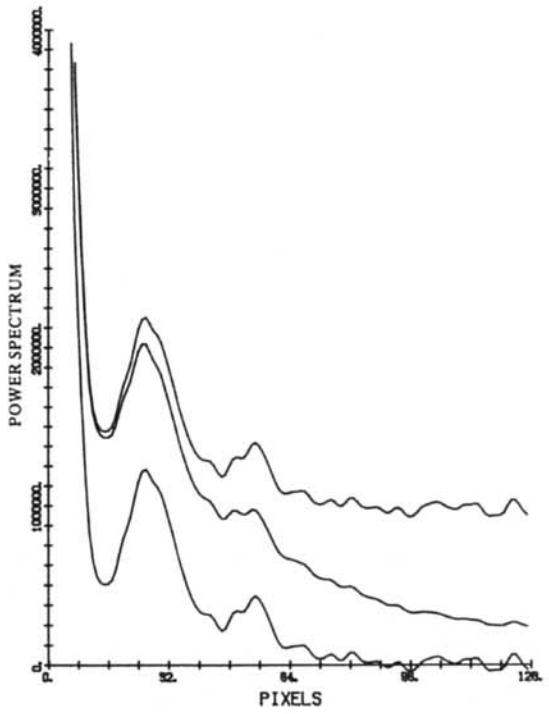

Figure 3. Power spectrum of the binary SAO 94163. (A) Middle curve: raw summed power spectrum; (B) upper curve: summed power spectrum divided by the DTF^2; (C) lower curve: DTF^2 - compensated summed power spectrum with noise bias subtracted.

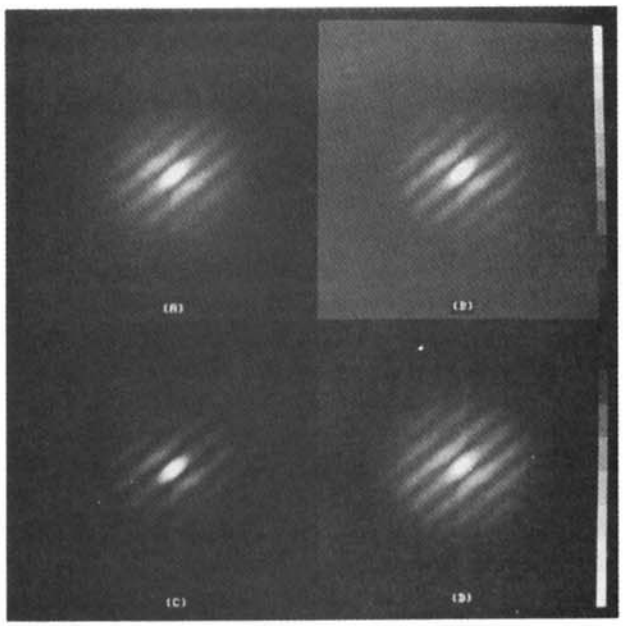

Figure 4. (A)-(C) Two dimensional view of Figure 3(A)-(C); (D) the Fourier modulus, i.e., the square root of (C). Note: the residual noise beyond the telescope cut-off frequency is visible in this case and not in (C) because the square root operation reduces the dynamic range of the data.

In some instances, there is not available the summed power spectrum of a reference star close enough in both space and time to the observation of the object. In that case, one approach is to approximate the actual speckle MTF^2 by fitting a model[9] of the speckle MTF^2 to the data. Another alternative is the Worden subtract method[13]. There seems to be some controversy over the effectiveness of this method[14]; there is no doubt that it provides a much better estimate of the object's power spectrum than the summed power spectrum, but further investigation is needed to determine whether it is the best available estimate.

The Worden subtract method of compensating for the speckle MTF^2 consists of subtracting from the summed autocorrelation the sum of cross-correlations of different short-exposure images. The short-exposure images must be centroided before being cross-correlated[15]. It is easily shown that subtraction of a properly scaled version of the power spectrum of the sum of the centroided images from the summed power spectrum is exactly equivalent to the Worden subtract method. Figure 5(a) shows a cut through these two functions for very low spatial frequencies for the unresolved star SAO 36615. Both are similar in their spike-like behavior for very low spatial frequencies. However, for spatial frequencies at four pixels from zero frequency and beyond, the power spectrum of the sum of the centroided images is essentially zero. Thus, it would appear that the Worden subtract method could correct only for the very lowest spatial frequencies. This is borne out in Figures 5(b) and 5(c). Furthermore, recalling that the compensated summed power spectrum for an unresolved star should be a constant (weighted by the MTF^2 of the telescope aperture which is nearly unity for these very low spatial frequencies), we see from Figures 5(b) and (c) that the Worden subtract method did not produce the expected result. By getting rid of most of the low-frequency spike in the summed power spectrum, the Worden subtract method did greatly decrease its mean-squared error; however, it did not replace the spike with the correct low-frequency information. It is not presently known whether this apparent inadequacy of the Worden subtract method is due to basic inadequacies of the method itself or due to problems with this particular data set; however, it is consistent with the analysis of Fante[14].

A better speckle MTF^2 compensation than the Worden subtract method in this case would simply be to clip the summed power spectrum at the very low spatial frequencies. That is, assuming that the object's power spectrum is nearly constant for the very low spatial fre-

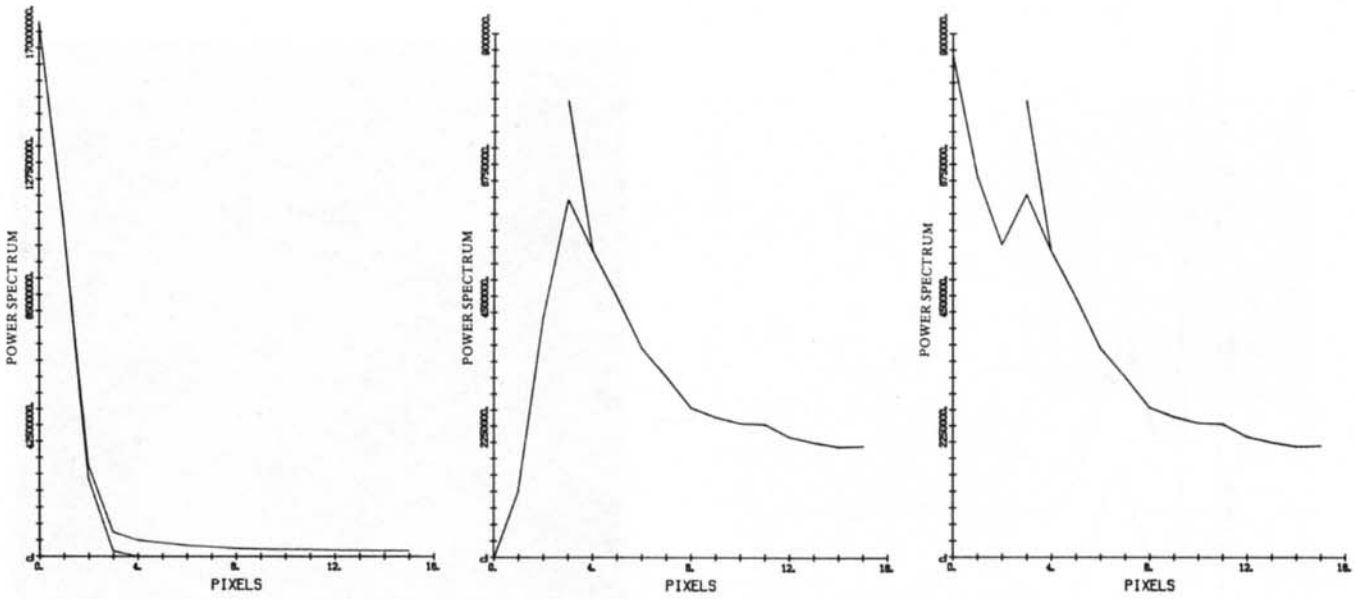

Figure 5. Worden subtract method on an unresolved star (low spatial frequencies). (A) upper curve: summed power spectrum; lower curve: power spectrum of the sum of the centroided images; (B) upper curve: summed power spectrum (note expanded vertical scale); lower curve: summed power spectrum minus the power spectrum of the sum of the centroided images; (C) same as (B), except a smaller percentage of the power spectrum of the sum of the centroided images was subtracted.

quencies (which would be true for objects of diameter only a small fraction of an arc-sec), we replace the summed power spectrum in that region by a constant. The constant is chosen to be consistent with the value of the summed power spectrum in the region just beyond the very low-frequency spike. As in this case of the Worden subtract method, this method does not correct for the middle-frequency vs. higher-frequency regions of the speckle MTF^2; however, as noted earlier, the speckle MTF^2 is reasonably well behaved for those spatial frequencies, and correcting for the very low spatial frequencies corrects for the greatest part of the error.

The method of clipping the summed power spectrum to correct for the speckle MTF^2 is demonstrated in Figure 6 for the binary SAO 94163 for which reference star data was not available. In order to increase the accuracy of the assumption that the Fourier modulus (or its square, the power spectrum) is constant for very low spatial frequencies, the DTF and noise-bias-corrected Fourier modulus was divided by the MTF due to the telescope aperture (which was approximated by the MTF due to a circular aperture of diameter 2.3 meters). The elliptical shape of the Fourier modulus data is due to the difference in scale factors in the two dimensions as noted earlier. Within the low frequency region, wherever the Fourier modulus exceeded a threshold value, it was clipped to that threshold value. The result was multiplied by the MTF due to the telescope to arrive at our final estimate of the Fourier modulus of SAO 94163 including the telescope MTF. In the process of multiplying back in the telescope MTF, the residual noise beyond the telescope cut-off frequency was set to zero.

Image reconstruction results

The Fourier modulus estimate shown in Figure 6(d) was truncated to a 128 x 128 array, in order to save computation time in the iterative reconstruction. This caused a slight truncation of the highest spatial frequencies along the horizontal dimension of Figure 6(d). SAO 94163 was reconstructed using the iterative method, and the images resulting from two different selections of the initial input to the algorithm are shown in Figures 7(a) and (b), respectively. The rms error E_o was reduced to about 0.05. For the purpose of display, a (sin x)/x interpolation was performed on the images of Figure 7 in order to increase the sampling rate across the image. In order to get an indication of the sensitivity of the method to the clipping threshold level described in the previous section, the clipping was done over again using a 33% greater threshold value (which is obviously greater than the optimum threshold). Two images reconstructed from the resulting Fourier modulus estimate are shown in Figure 7(c) and (d). Half the time, the iterative reconstruction algorithm produces an image rotated by 180° due to the inherent 2-fold ambiguity of the Fourier modulus data.

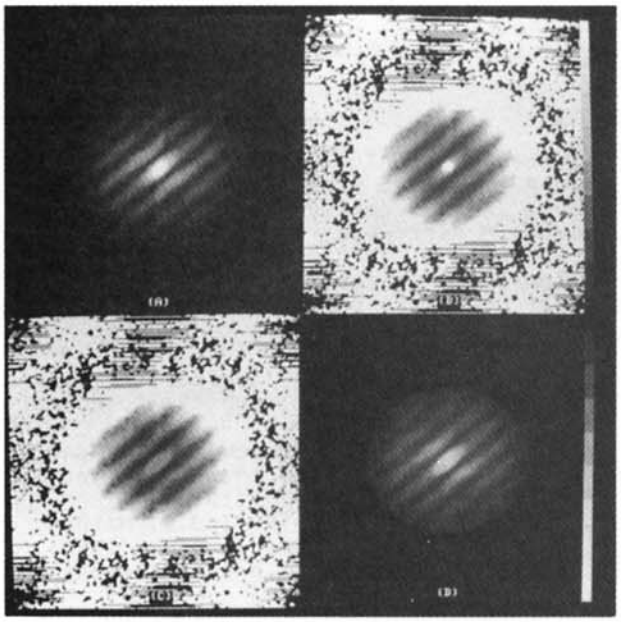

Figure 6. Clipping to compensate for the speckle MTF (for "seeing") for the binary SAO 94163. (A) Fourier modulus, same as Figure 4(D); (B) Fourier modulus compensated for telescope MTF (attempted division by zero is evident for spatial frequencies above the telescope cut-off frequency); (C) clipping of the low spatial frequencies; (D) Fourier modulus estimate obtained by putting back in the telescope MTF.

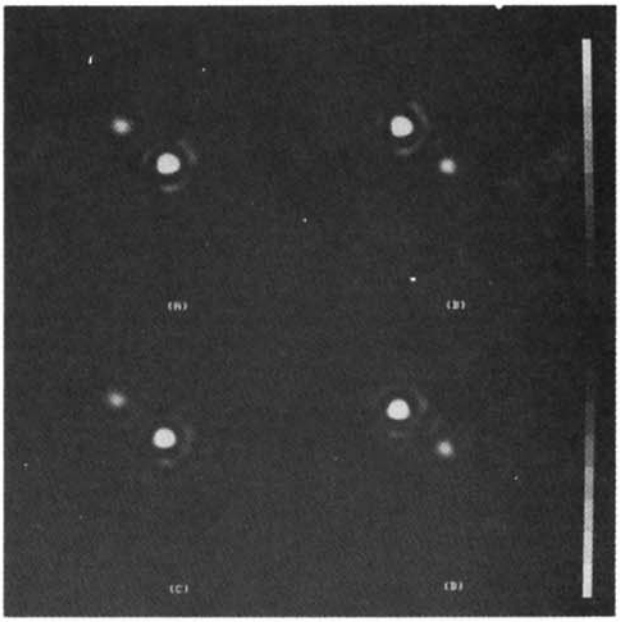

Figure 7. Reconstructed images of SAO 94163 (see text).

The average separation of the reconstructed images is 13.9 pixels ≈ 0.27 arc-sec and the orientation angle is 42.7° (47.3° from the orthogonal axis). The brightness ratios, based on the maximum brightness of each star in the pair, are 4.38, 4.17, 4.14, and 3.96 for Figures 7(a) through (d), respectively, and the corresponding magnitude differences are 1.60, 1.55, 1.54, and 1.49, respectively. Thus, a 33% increase in threshold level caused only a 6% decrease in the computed brightness ratio. The average magnitude difference of the reconstructions of Figures 7(a) and (b) is 1.57.

Conclusions

We have discussed steps necessary to obtain an accurate estimate of an object's Fourier modulus from the raw summed power spectrum: detection transfer function compensation, noise bias subtraction, and speckle MTF compensation. For compensation of the speckle MTF when reference star data is not available, an improvement over the Worden subtract method is the simple method of clipping the Fourier modulus spike at the very low spatial frequencies (for objects much smaller than one arc-sec in diameter). A reconstruction of the binary SAO 94163 using this method resulted in an image having a binary separation of 0.27 arc-sec at an angle of 42.7° (47.3°) and a magnitude difference of 1.57 (brightness ratio of 4.26). The reconstruction of a binary is trivial and does not require the use of the iterative method; however, the iterative method is required for complicated objects, and the data processing steps described here for this simple example can be used in more general circumstances. Based on the success of image reconstruction experiments using summed power spectra of complicated two-dimensional objects computer-simulated to include the effects of atmospheric turbulence and photon noise[11], it is expected that it will be possible to reconstruct fine-resolution images of complicated astronomical objects.

Acknowledgements

We gratefully acknowledge the helpful suggestions of K. Hege and thank him and his colleagues at Steward Observatory for sharing this stellar speckle interferometry data with us. Programming assistance by C. Roussi is also acknowledged. This work was supported by the Air Force Office of Scientific Research under Contract No. F49620-80-C-0006.

References

1. A. Labeyrie, "Attainment of Diffraction Limited Resolution in Large Telescopes by Fourier Analysing Speckle Patterns in Star Images," Astron. and Astrophys. 6, 85 (1970); D.Y. Gezari, A. Labeyrie, and R.V. Stachnik, "Speckle Interferometry: Diffraction-Limited Measurements of Nine Stars with the 200-inch Telescope," Astrophys. J. Lett. 173, L1 (1972).

2. C.Y.C. Liu and A.W. Lohmann, "High Resolution Image Formation through the Turbulent Atmosphere," Opt. Commun. 8, 372 (1973); G.P. Weigelt, "Stellar Speckle Interferometry and Speckle Holography at Low Light Levels," Proc. SPIE 243-17, Applications of Speckle Phenomena (July 1980).

3. J.R. Fienup, "Reconstruction of an Object from the Modulus of Its Fourier Transform," Opt. Lett. 3, 27 (1978); J.R. Fienup, "Space Object Imaging through the Turbulent Atmosphere, Opt. Eng. 18, 529 (1979).

4. K.T. Knox and B.J. Thompson, "Recovery of Images from Atmospherically Degraded Short-Exposure Photographs," Astrophys. J. Lett. 193, L45 (1974); J.W. Sherman, "Speckle Imaging Using the Principal Value Decomposition Method," Proc. SPIE 149 (1978).

5. Special issue on Adaptive Optics, J. Opt. Soc. Am. 67, March 1977; J.W. Hardy, "Active Optics: A New Technology for the Control of Light," Proc. IEEE 66, 651 (1978).

6. J.R. Fienup, "Iterative Method Applied to Image Reconstruction and to Computer-Generated Holograms," Opt. Eng. 19, 297 (1980).

7. P.A. Strittmatter, "The Steward Observatory Speckle Interferometry Program," Proc. SPIE 243-12, Applications of Speckle Phenomena (July 1980).

8. J.W. Goodman, Introduction to Fourier Optics (McGraw-Hill, San Francisco, 1968), p. 119.

9. D. Korff, G. Dryden, and M.G. Miller, Opt. Commun. 5, 187 (1972).

10. J.W. Goodman and J.F. Belsher, "Fundamental Limitations in Linear Invariant Restoration of Atmospherically Degraded Images," Proc. SPIE 75, Imaging through the Atmosphere (1976), p. 141; J.C. Dainty and A.H. Greenaway, "Estimation of Power Spectra in Speckle Interferometry," J. Opt. Soc. Am. 69, 786 (1979).

11. G.B. Feldkamp and J.R. Fienup, "Noise Properties of Images Reconstructed from Fourier Modulus," Proc. SPIE 231-08, 1980 International Optical Computing Conference (April 1980).

12. C. Aime, S. Kadir, G. Ricort, C. Roddier, and J. Vernin, "Measurements of Stellar Speckle Interferometry Lens-Atmosphere Modulation Transfer Function," Optica Acta 26, 575 (1979).

13. S.P. Worden, M.K. Stein, G.D. Schmidt, and J.R.P. Angel, "The Angular Diameter of Vesta from Speckle Interferometry," Icarus 32, 450 (1977); G. Welter and S.P. Worden, "A Method for Processing Stellar Speckle Data," J. Opt. Soc. Am. 68, 1271 (1978).

14. R.L. Fante, "Comments on a Method for Processing Stellar Speckle Data," J. Opt. Soc. Am. 69, 1394 (1979).

15. S.P. Worden and M.K. Stein, "Angular Diameter of the Asteroids Vesta and Pallas Determined from Speckle Observations," Astronomical J. 84, 140 (1979).